

## Modeling studies of amorphous carbon

D. Beeman,\* J. Silverman, R. Lynds, and M. R. Anderson  
*Physics Department, Harvey Mudd College, Claremont, California 91711*  
(Received 9 January 1984)

Three structural models of amorphous carbon with differing percentages of threefold- and fourfold-coordinated atoms were constructed and analyzed, along with a purely four-coordinated amorphous Ge model which was scaled to diamond bond lengths. The radial distribution function and interference function,  $F(k)$ , of the model containing 14% four-coordinated atoms were in best agreement with the experimental results of Boiko *et al.*, although the functions containing 48% four-coordinated atoms were in best agreement with the results of Kakinoki *et al.* The unavoidable planar nature of the entirely three-coordinated model caused its  $F(k)$  to be in poor agreement with experiment. Raman and vibrational density-of-states (DOS) spectra were also calculated for the models. The presence of disorder in the three-coordinated model produced a downward shift in frequency of the principal Raman peak and DOS band edge from the position seen in graphite. With the addition of four-coordinated atoms, there was a gradual transition from graphitelike spectra to diamondlike spectra, rather than spectra with a mixture of distinct features typical of graphite and diamond. In addition, there was a further downward shift in frequency of the main Raman peak and in that of the "disorder peak" seen in microcrystalline and amorphous carbon. The spectra of the model containing 14% four-coordinated carbon was in best agreement with recent Raman scattering experiments. These results suggest a structure for amorphous carbon consisting of three-coordinated planar regions with occasional four-coordinated atoms allowing changes in orientation of the planes. The positions of the peaks in the spectra suggest that the proportion of four-coordinated atoms is not likely to exceed 10%.

### I. INTRODUCTION

Amorphous carbon (*a*-C) has a much greater hardness<sup>1</sup> and mechanical strength<sup>2</sup> than graphite and has a pseudogap and a hopping conductivity very similar to that of other amorphous semiconductors.<sup>3</sup> The first step towards an understanding of the mechanical and electrical properties of *a*-C is to develop a satisfactory model of the structure. Although there is considerable evidence suggesting that the structure of *a*-Si and *a*-Ge is a randomly connected network of tetrahedrally bonded atoms, there is much less agreement as to the structure of *a*-C. Studies of the radial distribution function (RDF) obtained from electron-diffraction experiments have in some cases suggested that the bonding is entirely three coordinated, as in graphite,<sup>4</sup> and in others have been interpreted to indicate that as much as 50% diamondlike tetrahedral bonding may be present.<sup>5</sup> Electron-energy-loss spectra obtained by Batson and Craven<sup>6</sup> indicated graphitic bonding in one sample, whereas another sample showed a structure suggesting tetrahedral coordination. From analysis of their neutron-diffraction data, Mildner and Carpenter<sup>7</sup> conclude that the percentage of tetrahedrally bonded atoms in *a*-C is no more than 10% and is probably less than 5%. Recent Raman scattering experiments show a spectrum which is much closer to that of graphite than of diamond.<sup>1,8-10</sup>

Much of our knowledge of the structure of *a*-Si and *a*-Ge has been obtained by constructing physical models with several hundred atoms and calculating the RDF of the model structures.<sup>11</sup> As the RDF does not uniquely

specify the structure, it is necessary to calculate other properties, such as the Raman and infrared-absorption spectra, as well.<sup>12,13</sup> In order to better understand the structure of *a*-C, we present here an analysis of the structure and vibrational properties of several models of *a*-C.

### II. DESCRIPTION OF THE MODELS

During the course of this study, three large structural models of amorphous carbon were built by hand. One model, consisting of 1120 atoms (hereafter referred to as the C1120 model), is entirely three coordinated. Another (the C356 model), built to test the hypothesis of Kakinoki *et al.*,<sup>5</sup> contains 356 atoms of which 51% are tetrahedrally coordinated. Studies of these two models suggested a need for the third (the C340 model), containing 340 atoms with 9% tetrahedral bonding. An interior sphere of fully bonded atoms was used in the calculation of the RDF and the vibrational spectra of these models. In this region, the C356 model has 48% four-coordinated atoms and the C340 model has 14% four-coordinated atoms. For purposes of comparison, a fourth model having 100% tetrahedral coordination (C519) was generated by rescaling the 519-atom Polk model<sup>11</sup> of amorphous germanium. Although this model is not considered as a likely candidate for the structure of *a*-C, it provides some useful insight into the trends which are observed when the percentage of four-coordinated atoms is varied. With the exception of the C1120 model, these are relatively isotropic randomly connected networks with no interior dangling bonds. Significant numbers of five- and seven-membered

TABLE I. Summary of structural properties of models.

Model	Four-coordinated atoms		Rings per atom			
	(%)	$\theta_3$ (deg)	$\theta_4$ (deg)	Fivefold	Sixfold	Sevenfold
C1120	0	117.7 $\pm$ 5.0		0.106	0.294	0.100
C340	9.1	117.3 $\pm$ 5.9	108.9 $\pm$ 6.2	0.055	0.329	0.119
C356	51.4	116.9 $\pm$ 7.1	109.9 $\pm$ 7.1	0.098	0.312	0.278
C519	100		109.4 $\pm$ 7.1	0.360	1.00	1.04

rings were incorporated into the structures, as well as a few eight- and nine-membered rings. No four-membered rings were used. As the C340 model is mostly three coordinated, with 120° bond angles, the short-range topology of the model is planar, with the small number of tetrahedrally coordinated atoms allowing the planes to be bent and interconnected. The resulting structure has little distortion in bond lengths and bond angles, yet has a fairly random orientation of planes. When the bonding is exclusively graphitic as in the case of the C1120 model, it is not possible to deviate from a flat planar structure without extreme distortions in bond angle. Therefore, the C1120 model was constructed from four stacked, slightly warped 280-atom planes. The four layers are topologically equivalent, as they are replicas of a single hand-built layer, rotated by 0°, 60°, 120°, and 270°. All models were computer relaxed by the method of Steinhardt *et al.*<sup>14</sup> to minimize the strain energy due to distortions in bond length and bond angle from their crystalline values. Thus, the target bond angles in the relaxation process were 120° for the three-coordinated atoms and 109.4° for four-coordinated atoms. Bond lengths between three-coordinated atoms were relaxed toward the 1.42 Å graphite bond length, bonds between four-coordinated atoms were relaxed toward the diamond bond length of 1.56 Å, and bonds between three-coordinated atoms and four-coordination atoms were relaxed toward the 1.51 Å distance found in toluene. In the relaxation of the C1120 model, an additional central-force interaction was used between nearest neighbors on adjacent planes in order to force their separation towards the 3.64 Å distance found in graphite. (Although the closest distance between atoms on adjacent graphite planes is 3.35 Å, 9 times as many pairs occur at a spacing of 3.64 Å.) The ring statistics, average bond angles and rms deviations, and the percentage of interior tetrahedrally coordinated atoms for the four models are presented in Table I.

### III. RDF ANALYSIS

Radial distribution functions were calculated for an interior sphere of fully bonded atoms in each of the models. The RDF's were corrected for the finite size of the models and were Gaussian broadened to fit the width of the first peak in the experimental RDF's, which has been broadened to minimize termination effects. Although this method of display tends to suppress details in the model RDF, it is useful because it helps to answer the important question of whether the model is more or less disordered than the experimentally studied system. Figure 1 displays the RDF's of the C1120, C340, C356, and C519 models

(solid lines) along with the experimental results of Boiko *et al.*<sup>4</sup> (dashed lines) and of Kakinoki *et al.*<sup>5</sup> (dotted-dashed lines). Table II summarizes the positions of the first and second peaks in the RDF, the nearest-neighbor coordination numbers, and the densities calculated from these RDF's, as well as those of graphite and diamond.

From a visual inspection of the RDF's of Fig. 1 and a comparison of the calculated densities in Table II, it is apparent that all of the models except the exclusively three-coordinated C1120 model have a significantly higher density than the experimentally studied samples. The C340 model, being mostly three coordinated, could very likely have been built in a more open structure with a lower density. The high density of the C356 and C519 models is a more serious flaw in the models because the large number of tetrahedral bonds enforces a much more densely packed construction. Although it is difficult to imagine a completely tetrahedrally coordinated structure having a

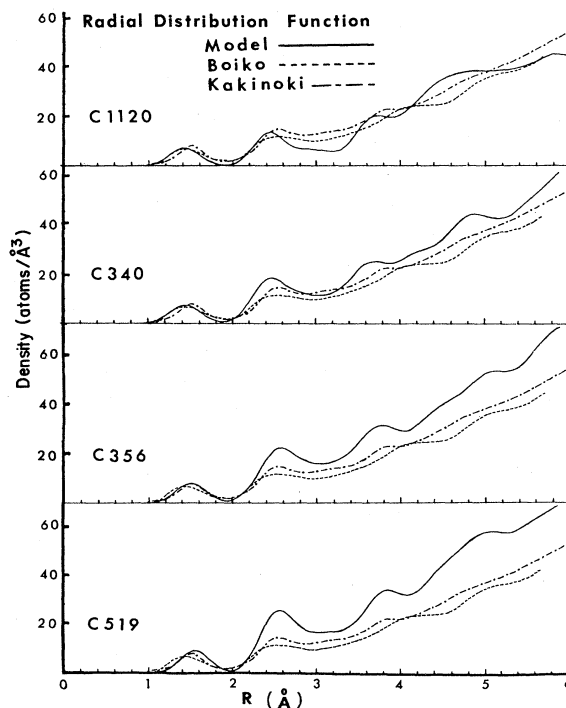


FIG. 1. Radial distribution functions calculated for the four models (solid lines) compared to the experimental RDF's of Boiko *et al.* (dashed lines) and Kakinoki *et al.* (dotted-dashed line).

TABLE II. Quantities calculated from the radial distribution function.

	$r_1$ (Å)	$r_2$ (Å)	$n_1$	$\rho$ (g/cm <sup>3</sup> )
	Model			
C1120	1.42	2.44	3.00	2.11
C340	1.42	2.43	3.28	2.69
C356	1.51	2.55	3.53	3.21
C519	1.55	2.52	4.00	3.39
	Experimental			
Boiko <sup>a</sup>	1.43	2.53	3.3	2.1
Kakinoki <sup>b</sup>	1.51	2.53	3.45	2.4
	Cluster models			
Graphite	1.42	2.45	3.00	2.25
Diamond	1.55	2.52	4.00	3.51

<sup>a</sup>See Ref. 4.

<sup>b</sup>See Ref. 5.

density very much less than that of diamond, it might be possible to decrease the density of a structure having roughly 50% tetrahedral coordination by using a less homogeneous distribution of three- and four-coordinated atoms than was used in the C356 model. Kakinoki *et al.* have suggested a model in which regions containing only three-coordinated atoms are bonded to regions containing only four-coordinated atoms. Such a structure, containing planar three-coordinated regions several angstroms across, could have large voids which would significantly reduce its density. There is also considerable uncertainty in the densities which were used to normalize the experimental RDF's. The density used by Kakinoki *et al.* was estimated from the dimensions and weight of the sample and did not take any porosity of the sample into account.<sup>5</sup> Boiko *et al.* used a value taken from the literature which may not have been appropriate for their sample, which was observed to have pores averaging 12 Å in size.<sup>4</sup>

The position of the first peak in the RDF of the C340 model is very close to the nearest-neighbor distance in graphite, as bonds between three-coordinated atoms are by far the most prevalent. This peak position and the coordination number calculated from the area under the peak are in good agreement with the results of Boiko *et al.*, although there is a large uncertainty in the experimentally measured coordination number. The majority of the bonds in the C356 model are between three-coordinated atoms and four-coordinated atoms, producing a peak at 1.51 Å. This peak position and the calculated coordination number are in agreement with the results of Kakinoki *et al.* However, this peak could also arise from a composite of the two peaks in the inhomogeneous model proposed by Kakinoki *et al.* The second peak, occurring at 2.52 Å in both experimental RDF's, falls at a significantly smaller value for the C1120 and C340 models, and occurs at approximately the correct position for the C356 and C519 models. A study of the unbroadened model RDF's (not shown here) reveals that in the C1120 model this peak arises mainly from 2.45 Å second-neighbor distance

in six-membered rings with significant contributions from the 2.30 and 2.56 Å second-neighbor distances in five- and seven-membered rings. In the remaining models, the many different types of distorted rings produce a fairly smooth distribution of second-neighbor distances. The third peaks in the RDF's of all of the models arises from a variety of distant neighbors, and are not in good agreement with experiment, although the models having the largest percentages of four-coordinated atoms are in best agreement with the results of Kakinoki *et al.*

It is also useful to examine the interference function, defined as

$$F(k) = \int_0^{\infty} [J(r)/r - 4\pi\rho r] \sin(kr) dr,$$

where  $J(r)$  is the RDF and  $\rho$  is the mean number density. This function is shown for the various models and experiments in Fig. 2. The most striking feature of the  $F(k)$  calculated for the C1120 model is the strong peak at  $1.72 \text{ \AA}^{-1} = 2\pi/(3.64 \text{ \AA})$ , which is not seen in the experimental data. This is a result of the unavoidable planar nature of the entirely three-coordinated model with its periodic 3.64-Å separation between neighboring atoms on different planes. As is the case with the calculated RDF's, the interference function for the Boiko *et al.* experiment is best fitted by the C340 model and that of Kakinoki *et al.* is best fitted by the C356 model, with its larger percentage of four-coordinated atoms. In spite of the great difference between the structure of the C519 model and the others, the RDF's are rather similar. This suggests the need for the analysis of other experimental quantities which are

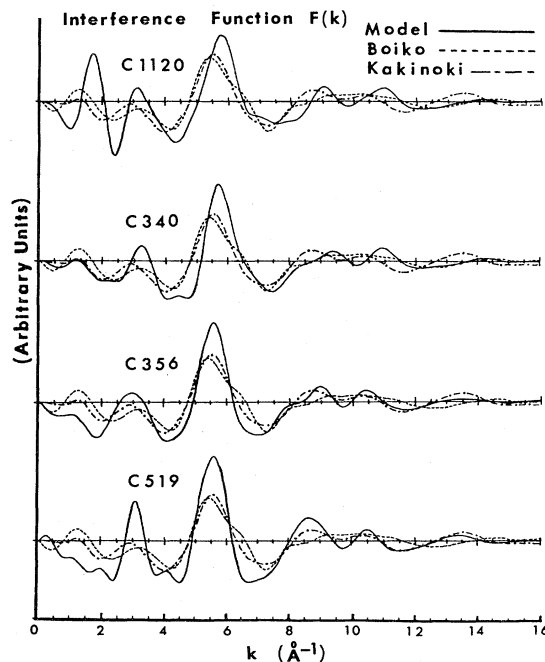


FIG. 2. Interference functions calculated for the four models (solid lines) compared to the experimental RDF's of Boiko *et al.* (dashed line) and Kakinoki *et al.* (dotted-dashed line).

sensitive to the structure, such as the vibrational spectrum.

#### IV. VIBRATIONAL PROPERTIES

The vibrational densities of states (DOS's) and Raman spectra of the models were calculated using the equation-of-motion method.<sup>13</sup> The force constants used in the vibrational calculations were taken from simple force models which represent the main features of the graphite and diamond spectra, correctly giving the frequency of the main high-frequency Raman peak and giving the best compromise for the general shape of the rest of the DOS spectrum. For graphite, a valence-force-field (VFF) model was used with nearest-neighbor bond-stretching and -bending forces, in addition to an out-of-plane force.<sup>15</sup> These three force constants were chosen to be 363, 36, and 134 N/m, respectively. A two-parameter VFF model with a bond-stretching force constant of 270 N/m and a bond-bending force constant of 25 N/m was used to fit the  $1332\text{-cm}^{-1}$  Raman peak occurring at the upper edge of the diamond DOS. The force constant for stretching of bonds between three- and four-coordinated atoms was taken to be the average of the graphite and diamond bond-stretching constants.

The vibrational spectrum of a model is calculated from the Fourier transform of the time-dependent self-correlation function of its atomic displacements. When the initial displacements from equilibrium are chosen randomly, the resulting spectrum is the full vibrational DOS. Initial conditions which select Raman-active modes of vibration are obtained using three phenomenological mechanisms [ $R(1)$ ,  $R(2)$ , and  $R(3)$ ] which correspond to symmetry-allowed contributions to the polarizability from pairs of atoms.<sup>12,13</sup>  $R(1)$  is a bond-stretching mechanism which contributes chiefly to the high-frequency part of the spectrum.  $R(2)$ , which involves the rocking of bonds, gives the major contribution to the lower-frequency part of the Raman spectrum. These two mechanisms contribute to both the maximally depolarized spectrum  $HV$  and the polarized spectrum  $HH$ .  $R(3)$  is a bond-stretching mechanism which contributes only to polarized Raman scattering. As the  $HV$  and  $HH$  spectra of  $a\text{-C}$  are very similar,<sup>16</sup> and the model spectra calculated using  $R(3)$  had no strong features, the reduced Raman spectrum of a model was represented by a weighted average of the spectra calculated using  $R(1)$  and  $R(2)$ . For each model, the weighting was chosen to fit the height of the high-frequency peak of the experimentally measured<sup>8</sup> reduced Raman spectrum of  $a\text{-C}$  and the average level of the low-frequency part of the spectrum. As long-range forces are known to be important in both graphite and diamond, it is likely that other mechanisms involving nonbonded atoms may also contribute to the Raman spectrum. For this reason, it is useful to examine the DOS of the models, as it may reveal Raman-active features which are not reproduced by these simple mechanisms. For many amorphous materials, the reduced Raman  $HV$  spectrum, scaled by dividing by the frequency, approximates the DOS over most of its range.<sup>17</sup>

Figure 3 shows the DOS spectra of the four models and cluster models of graphite and diamond compared with

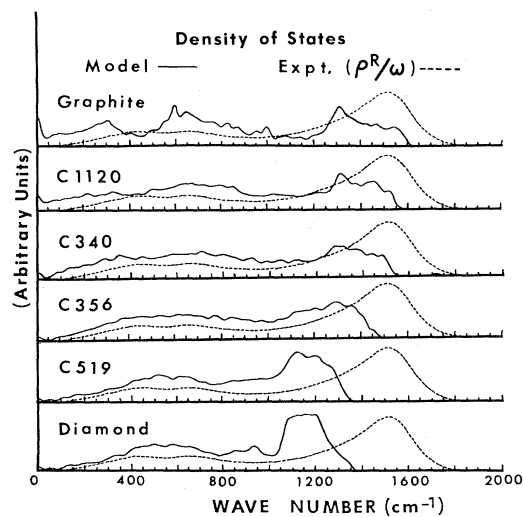


FIG. 3. Vibrational density-of-states spectra (solid lines) of the four amorphous carbon models and cluster models of graphite and diamond. The dashed lines represent the experimental reduced Raman spectrum from Ref. 8 divided by frequency in order to approximate the DOS.

Lannin's<sup>8</sup>  $a\text{-C}$  reduced Raman spectrum, which was divided by frequency to approximate the DOS. The calculated reduced Raman spectra of the models are compared to Lannin's experimental results in Fig. 4. A damping term was introduced in the Fourier transform to minimize oscillations arising from the finite time span of the integration of the equations of motion. This results in a broadening of the spectra, giving a resolution of  $29\text{ cm}^{-1}$  (full width at half maximum). The calculated Raman spectrum of the graphite model consisted of a single peak

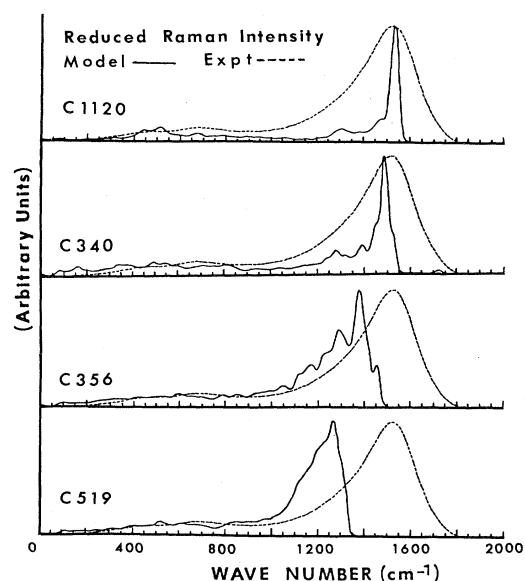


FIG. 4. Reduced Raman intensity calculated for the four models (solid lines) compared to the experimental results of Ref. 8 (dashed lines).

at  $1591\text{ cm}^{-1}$ , close to the experimentally observed value of  $1581\text{ cm}^{-1}$ . The diamond-like Raman peak occurs at the experimentally observed value of  $1332\text{ cm}^{-1}$ . For both of these crystalline models, the Raman peak occurs at the upper edge of the DOS spectrum.

The spectra of the C1120 model show the effects of bond-angle distortion accompanied by a decrease in the average bond angle and of the change in connectivity due to the addition of other than six-membered rings. Here we see a downward shift in the frequency of the principal Raman peak to  $1528\text{ cm}^{-1}$  and a corresponding shift in the upper edge of the DOS. In Lannin's Raman spectrum, this peak occurs slightly lower in frequency, at about  $1516\text{ cm}^{-1}$ . Both the Raman and DOS spectra of this model show only a hint of the pronounced dip occurring at  $440\text{ cm}^{-1}$  in the graphite-model DOS. This dip occurs at about  $560\text{ cm}^{-1}$  in calculations of the graphite DOS using more sophisticated force models.<sup>18</sup> Lannin's spectra also show a noticeable dip at about  $560\text{ cm}^{-1}$ , suggesting that *a*-C may be slightly more ordered than the C1120 model. If this is so, disorder alone may not be enough to account for the downward shift in frequency of the principal Raman peak.

The spectra of the C340, C356, and C519 models show the additional effects of adding tetrahedrally coordinated atoms. We see a gradual transition from graphitelike spectra to diamondlike spectra as four-coordinated atoms are incorporated into the structure, rather than spectra with a mixture of distinct features typical of graphite and diamond. In addition, there is a further downward shift in the frequency of the main Raman peak, roughly proportional to the percentage of four-coordinated atoms. For these three models, the peaks occur at 1489, 1374, and  $1265\text{ cm}^{-1}$ , respectively.

The graphite-model and C1120 DOS's as well as the C1120 Raman spectrum, show a peak at  $1310\text{ cm}^{-1}$  which we identify with the disorder peak seen at  $1355\text{ cm}^{-1}$  in microcrystalline graphite<sup>19</sup> and in annealed *a*-C films.<sup>1,9,10</sup> This feature in the DOS becomes Raman active due to the loss of long-range translational symmetry arising from dangling bonds in microcrystalline graphite or from disorder in *a*-C. In the C340 model with 14% four-coordinated atoms, this peak is shifted downwards to  $1278\text{ cm}^{-1}$ . Dillon *et al.*<sup>10</sup> find that this feature occurs at about  $1283\text{ cm}^{-1}$  in their as-deposited *a*-C films. Upon annealing, the line sharpens and shifts toward  $1353\text{ cm}^{-1}$ . This suggests that *a*-C may contain a small percentage of tetrahedral bonds which are broken upon annealing.

As is the case with the experimental Raman spectrum, the Raman spectra of the models have an asymmetric main peak with the greater weight occurring on the low-frequency side. A spectrum intermediate between the Raman and DOS spectra of either the C1120 or C340 model would give better agreement with experiment, suggesting that mechanisms for Raman activity other than the ones considered here could be important. To adequately fit the experimental spectrum on the high side of the peak, the model spectra would have to extend out to  $1800\text{ cm}^{-1}$ . Although increasing bond-angle distortion in models of *a*-Ge tends to broaden the high-frequency DOS peak on both sides,<sup>13,20</sup> this is not the case with three-coordinated

*a*-C, as may be seen from a comparison of the calculated graphite-model and C1120-model DOS's. This is most likely because any deviation from the planar graphite structure towards a puckered structure lowers the average bond angle, rather than producing a symmetric distribution of bond angles about the crystalline value. The failure of the model calculations to give the correct position of the upper edge of the Raman spectrum could be due to the simplified force model used, which includes only interactions between nearest neighbors. The existence of a small number of two-coordinated carbon atoms, as in acetylene, could also extend the Raman spectrum upwards in frequency, as this double bond would be much stronger than the graphitic bond. Either of these possibilities could also compensate for the decrease in the frequency of the upper band edge caused by the inclusion of four-coordinated atoms.

## V. CONCLUSIONS

The above analysis of the vibrational spectra of the models leads us to conclude that *a*-C is primarily three-coordinated and that the percentage of tetrahedrally coordinated carbon, if any, is probably less than 10%. The positions of the principal Raman peak and the disorder peak in *a*-C relative to their frequencies in graphite suggests that there may be a small (5–10%) amount of tetrahedral bonding present, however.

The analysis of the densities of the models and the comparisons of their RDF's and interference functions with the experimental results of Boiko *et al.* also lead to the conclusion that *a*-C is primarily three coordinated. On the other hand, the RDF of Kakinoki *et al.* is in best agreement with models having a large percentage of tetrahedrally coordinated atoms. Mildner and Carpenter<sup>7</sup> suggest that Kakinoki's use of the macroscopic density to normalize the data from thin films may have led to incorrect results. If these results were correct, and the samples studied by Kakinoki *et al.* had 50% tetrahedral coordination, one would expect similar samples to have Raman spectra considerably different from those reported in Refs. 1 and 8–10. This is unlikely, as the samples used in these Raman studies were prepared by a variety of methods, including the evaporation method used by Kakinoki, and the spectra were all quite similar. It has been pointed out<sup>1</sup> that, as the Raman scattering efficiency of diamond is much less than that of graphite, the contribution from tetrahedral bonds might not be noticeable. This would likely be true for an inhomogeneous structure having large diamondlike regions connected by large graphitic regions. However, we have seen that when the tetrahedrally bonded atoms are uniformly distributed throughout the model, the effect is to modify the vibrational spectrum of the model as a whole, rather than to introduce spectral features typical of scattering from "diamond atoms."

Perhaps the strongest argument for the presence of some tetrahedral bonding in *a*-C is the lack of agreement between the interference function for the necessarily highly anisotropic layered structure forced by pure threefold coordination, and the interference functions derived from

electron-diffraction studies of *a*-C. Wada *et al.*<sup>1</sup> have suggested a structure consisting of randomly oriented planes of amorphous three-coordinated carbon about 20 Å in diameter, having dangling bonds at the edges. This model is appealing, as it is isotropic, yet it does not involve the assumption of tetrahedral bonding. However, the density of the fully connected C1120 layered model is approximately correct, and a completely three-coordinated model with randomly oriented planes would surely have a much lower density. Furthermore, the weak attractive forces between planes would cause such a model to collapse into a layered structure unless the planes were connected by tetrahedrally coordinated atoms. It seems more reasonable to assume that the structure is similar to the C340 model, consisting of three-coordinated planar regions with occasional four-coordinated atoms allowing changes in orientation of the planes. This is likely to be energetically more favorable than a structure containing a large number of dangling bonds. The existence of tetrahedral bonding in *a*-C seems reasonable because any

bending or warping of planar regions of three-coordinated carbon would change the distance between the out-of-plane *p* orbitals and destroy the energetic advantage of *sp*<sup>2</sup> hybridization. Using electron microscopy, Iijima<sup>21</sup> has detected tetrahedral bonds in bent graphite layers within graphitized carbon particles. From the results of Wada *et al.* and Dillon *et al.* it seems that upon annealing, the short-range order more closely resembles crystalline graphite and the energetic advantage of tetrahedral bonding disappears, causing the tetrahedral bonds to break, allowing the formation of graphite microcrystals.

#### ACKNOWLEDGMENTS

We would like to thank C. Morse for valuable discussions on carbon bonding. We have also benefited from discussions with J. Lannin and S. A. Solin, and with R. O. Dillon and J. A. Woollam, who kindly provided unpublished experimental results. This research was supported by grants from the Research Corporation.

\*Corresponding author.

<sup>1</sup>N. Wada, P. J. Gaczi, and S. A. Solin, *J. Non-Cryst. Solids* **35-36**, 543 (1980).

<sup>2</sup>D. E. Bradley, *Br. J. Appl. Phys.* **5**, 65 (1954).

<sup>3</sup>J. J. Hauser, *Solid State Commun.* **17**, 1577 (1975); *J. Non-Cryst. Solids* **23**, 21 (1977).

<sup>4</sup>B. T. Boiko, L. S. Palatnik, and A. S. Derevyanchenko, *Dokl. Akad. Nauk SSSR* **179**, 316 (1968) [*Sov. Phys.—Dokl.* **13**, 237 (1968)].

<sup>5</sup>J. Kakinoki, K. Katada, T. Hanawa, and T. Ino, *Acta Crystallogr.* **13**, 171 (1960).

<sup>6</sup>P. E. Batson and A. J. Craven, *Phys. Rev. Lett.* **42**, 893 (1979).

<sup>7</sup>D. F. R. Mildner and J. M. Carpenter, *J. Non-Cryst. Solids* **47**, 391 (1982).

<sup>8</sup>J. Lannin, in *Amorphous and Liquid Semiconductors*, edited by W. E. Spear (University of Edinburgh Press, Edinburgh, 1977), p. 110.

<sup>9</sup>S. A. Solin, N. Wada, and J. Wong, in *Proceedings of the 14th International Conference on Physics of Semiconductors*, edited by B. L. H. Wilson (IOP, Bristol, 1978), p. 721.

<sup>10</sup>R. O. Dillon, J. A. Woollam, and V. Katkanant, *Phys. Rev. B* **29**, 3482 (1984).

<sup>11</sup>D. E. Polk, *J. Non-Cryst. Solids* **5**, 365 (1971).

<sup>12</sup>R. Alben, D. Weaire, J. E. Smith, Jr., and M. H. Brodsky, *Phys. Rev. B* **11**, 2271 (1975).

<sup>13</sup>D. Beeman and R. Alben, *Adv. Phys.* **26**, 339 (1977).

<sup>14</sup>P. Steinhardt, R. Alben, M. G. Duffy, and D. E. Polk, *Phys. Rev. B* **8**, 6021 (1973).

<sup>15</sup>R. J. Nemanich, G. Lucovsky, and S. A. Solin, *Solid State Commun.* **23**, 117 (1977).

<sup>16</sup>J. S. Lannin (private communication); S. A. Solin (private communication).

<sup>17</sup>J. S. Lannin, *Phys. Rev. B* **15**, 3863 (1977).

<sup>18</sup>R. Nicklow, N. Wakabayashi, and H. G. Smith, *Phys. Rev. B* **5**, 4951 (1972).

<sup>19</sup>F. Tuinstra and J. L. Koenig, *J. Chem. Phys.* **53**, 1126 (1970).

<sup>20</sup>P. E. Meek, in *The Physics of Non-Crystalline Solids*, edited by G. H. Frischat (Trans Tech S. A., Aedermannsdorf, Switzerland, 1977), p. 586.

<sup>21</sup>S. Iijima, *J. Cryst. Growth* **50**, 675 (1980).